



HAL
open science

Identification of the Stress Intensity Factor of Carbon Cathode by Digital Image Correlation

Donald Picard, Luca Sorelli, Julien Rethore, Houshang Alamdari,
Marc-Antoine Baril, Mario Fafard

► **To cite this version:**

Donald Picard, Luca Sorelli, Julien Rethore, Houshang Alamdari, Marc-Antoine Baril, et al.. Identification of the Stress Intensity Factor of Carbon Cathode by Digital Image Correlation. *LIGHT METALS* 2017, Feb 2017, San Diego, United States. pp.1275-1280, 10.1007/978-3-319-51541-0_152 . hal-04670819

HAL Id: hal-04670819

<https://hal.science/hal-04670819v1>

Submitted on 20 Dec 2024

HAL is a multi-disciplinary open access archive for the deposit and dissemination of scientific research documents, whether they are published or not. The documents may come from teaching and research institutions in France or abroad, or from public or private research centers.

L'archive ouverte pluridisciplinaire **HAL**, est destinée au dépôt et à la diffusion de documents scientifiques de niveau recherche, publiés ou non, émanant des établissements d'enseignement et de recherche français ou étrangers, des laboratoires publics ou privés.



Distributed under a Creative Commons Attribution - NonCommercial 4.0 International License

Identification of the Stress Intensity Factor of Carbon Cathode by Digital Image Correlation

Donald Picard, Luca Sorelli, Julien Réthoré, Houshang Alamdari, Marc-Antoine Baril, and Mario Fafard

Crack propagation in carbon cathode used in the aluminium industry has been investigated through flexural tests on notched specimens. The main parameters of interest were the geometrical evolution of the crack and the stress intensity factor at the tip ends. The latter, in the case of interfacial fracture in two-dimensional geometries, can be related to normal (mode I) and shear (mode II) stresses. In this work, a new methodology has been applied which optically measures the crack tip displacement field by Digital Image Correlation. The stress intensity factors derived from the experimental data are consistent with results available in the literature. Furthermore, the preliminary results showed that characterizing the mode I (opening) only is somehow challenging due to the heterogeneity of such carbonaceous materials.

Keywords

Carbon • Cathode • Crack propagation • Digital image correlation • Stress intensity factor

Introduction

An Hall-Héroult aluminium electrolysis cell is composed of various structural materials such as refractory concrete, steel and carbon [1]. Carbon is mainly used in the fabrication of the electrodes, i.e. anodes and cathodes, since it is able to maintain good thermo-electromechanical properties at the operational temperature (960 °C) of a cell [2–6]. While the carbon anode (consumable electrode) has to be replaced every 26 days (this number may vary depending of the cell technology), the cathode, on the other hand, is a part of the

cell lining and is thus considered as a non-consumable electrode.

The life span of an electrolysis cell is strongly correlated to the cell lining one. Failures leading to the end of life of the cell are generally related to a lining failure and can be classified in two categories. The first one contains failures related to normal operation such as lining degradation (e.g. erosion of the cathode and chemical contamination of refractory by the electrolytic bath) [1]. The second one includes abnormal early failures of the lining leading to liquid bath leakage. These are generally correlated to the quality of the preheating phase of the cell used to slowly increase the temperature of the materials from room temperature (approximately 25 °C) to the operational one (960 °C). This is mainly done to avoid thermal shock of lining materials during the early stage operation of the cell, which include the pouring of molten cryolithe (bath).

As mentioned, the lining is composed of refractories, cathode blocks and other materials within a steel potshell each having different thermal expansion coefficients. Hence, mechanical stresses are induced in the lining when heated and failure occurs when stress levels exceed material

D. Picard (✉) · H. Alamdari · M.-A. Baril · M. Fafard
Aluminium Research Centre—REGAL, Université Laval, G1V
0A6 Québec, QC, Canada
e-mail: donald.picard@gci.ulaval.ca

L. Sorelli
Centre de Recherche Sur Les Infrastructures En Béton, Université
Laval, G1V 0A6 Québec, QC, Canada

J. Réthoré
LaMCoS Laboratory, Université de Lyon, F69621 Villeurbanne
Cedex, France

strengths. In addition to liquid leakage, the generation of cracks in the cathode blocks will reduce significantly the cell electrical efficiency and thus it must be avoided. It is thus imperative to well understand the behaviour of the carbon cathode block and, more importantly, when it reaches a critical state, i.e. cracking.

In this work, the cracking behaviour is characterized through the stress intensity factors (SIF) which has been calculated using displacement field obtained with a Digital Image Correlation method during four-point bending tests of notched cathode samples.

Materials and Methods

Stress Intensity Factors

Determination of material failure is generally based on failure criteria such as Mohr-Coulomb or von Mises. The choice of the criterion is highly dependent of the material microstructure (metals, ceramics, etc.). Once the material reaches the failure level, cracks will appear. The evolution of those cracks may be related to a stress intensity factor [7] used to predict the stress state near the end of the crack tip.

Three linearly independent cracking modes (Fig. 1) are used to define the crack state: opening (mode I), in-plane shear (mode II) and out-of-plane shear (mode III). In the present case, i.e. interfacial fracture in two-dimensional geometry, only the first two modes are of interest. However, the focus has been set on mode I only, i.e. crack opening.

The relationship between the load and the stress intensity factor varies with the loading case [9]. However, comparison between experimental results and analytical solutions will not be addressed in this paper.

Digital Image Correlation

Digital Image Correlation (DIC) techniques have been emerging to investigate the damage behaviour of different materials [10, 11]. In summary, it is a measurement technique

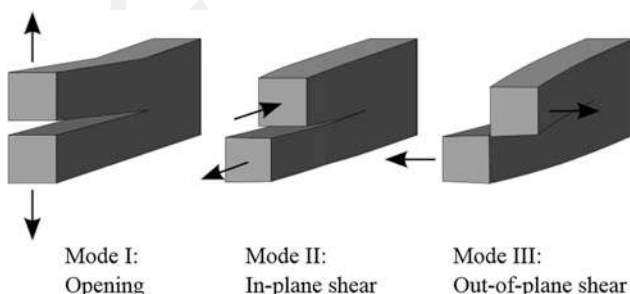


Fig. 1 Cracking modes in fracture mechanics. From [8]

that allows one to retrieve displacement fields “separating” two digital images of the same sample at different stages of loading. Because of its remarkable sensitivity, it is not only possible to detect cracks with sub-pixel opening, which would not be visible, but also to provide accurate estimates of stress intensity factors. For instance, in concrete science, DIC has been successfully applied to study the fracture mechanics of concrete, especially considering the crack opening [12] and the internal damage due to the expansive reaction of alkali reactive aggregates [13]. Recently, DIC analysis has been applied to study the microcrack process of Ultra High Performance Concrete (UHPC) during bending, which is a key to the structural ductility [14].

Cathode Samples

Cathode samples used for this study come from a graphitized carbon cathode. The compressive strength, tensile strength, Young’s modulus and Poisson’s ratio have been measured in laboratory according to ISO 18515:2007 [15] /ASTM C695-91 [16]/ASTM C469 [17]/ASTM C496 [18] standards and are available in Table 1.

The carbon cathode sample dimensions used for flexural tests (Fig. 2) were chosen according to ASTM C651 [19] standard and machined to the following values: 300 mm × 50 mm × 37.5 mm (Length × Height × Thickness). The initial notch height is 25 and 3 mm width. Also, as shown on Fig. 2, paint (black marks on a white background) was used on cathode samples for DIC purpose.

Flexural Tests

Flexural tests were done accordingly to the ASTM C651 [19] standard with a displacement rate of 0.2 mm/min. The apparatus used is schematized in Fig. 3 and was mounted on a MTS 810 loading frame. The distance between the upper cylindrical bearings was 70 and 210 mm between the bottom ones. The actuator displacement (LVDT) and load (MTS 5 kN load cell) were both recorded with a MTS FT40 controller. On the other hand, images used for DIC analysis were recorded with a mvBlueFox 102G camera at a rate of 50 frames/s.

Results and Discussion

Cracking Behavior

As highlighted in several studies (e.g. [2–6]) carbon cathode materials are highly heterogeneous. Hence, cracking path will be highly affected by this heterogeneity. In order to get a

Table 1 Mechanical properties of the graphitized carbon cathode

	Compressive strength (MPa)	Tensile strength (MPa)	Young's modulus (GPa)	Poisson's ratio
Value	11	1.8	2.05	0.03 ^a

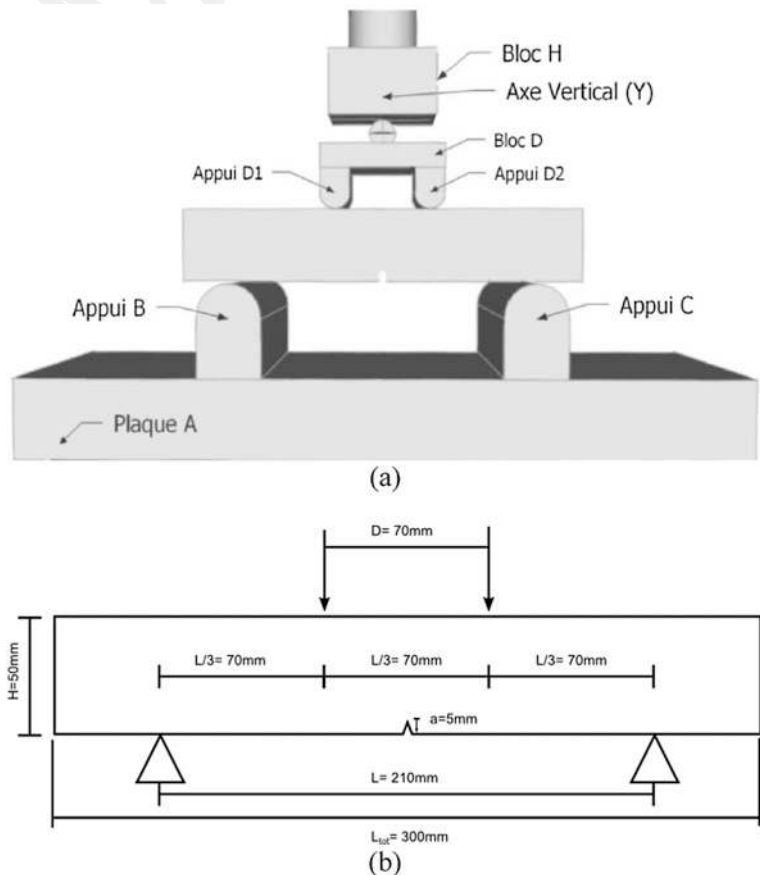
^aThe measurement error was very high on this parameter



Fig. 2 Typical carbon cathode sample used for stress intensity factor tests

representative behavior of mode I, cracking a large number of samples is thus required. Indeed, even though samples and notch geometries were selected in order to activate only the mode I, also shear behavior (mode II) has happened in several tests. Typical mode I and mode II cracking under four-point flexural test are shown in Figs. 4 and 5 respectively. However, as mentioned previously, this study has focused only on mode I as a first step.

Fig. 3 Scheme of the flexural apparatus: **a** setup; **b** dimension



Typically, mode I cracking will lead to the fully fractured sample shown in Fig. 6, which presents pictures of a sample at the end of the test. As shown on those pictures, the cracking pattern through the thickness of the sample is not the same one as the one observed with the DIC on the painted front face. This highlighted again the high influence of sample heterogeneity. In order to get two representative samples exhibiting mode I cracking behavior at least five tests have been performed. The two samples discussed in this paper are called SIF-I-01 and SIF-I-02, which are already been introduced in Fig. 4.

2D Displacement Field

The displacement results of samples SIF-I-01 and SIF-I-02 being similar, only one of them, sample SIF-I-01, will be discussed in this section and are presented in Figs. 7 and 8.

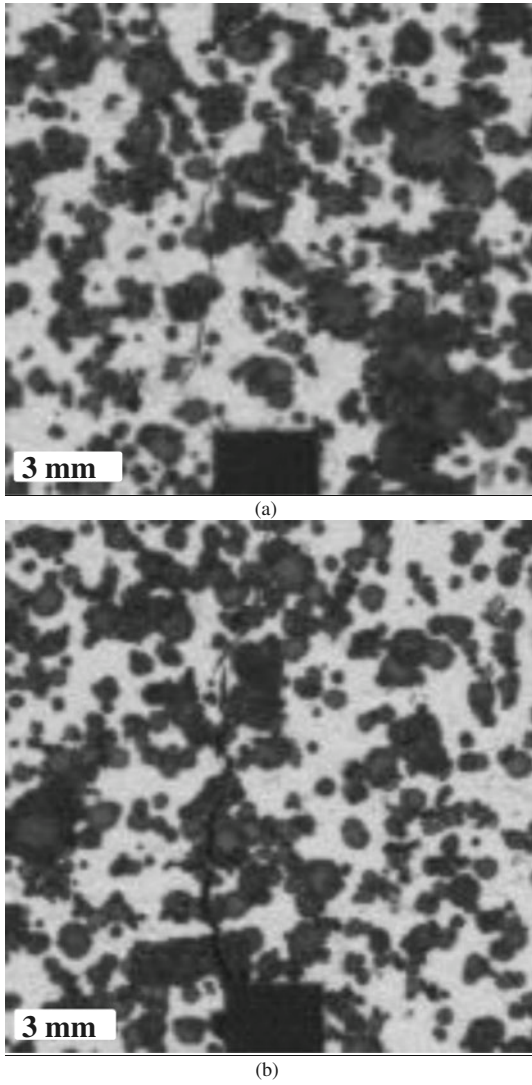


Fig. 4 Mode I crack pattern observed on painted graphitized carbon cathode: **a** sample SIF-I-01; **b** sample SIF-I-02

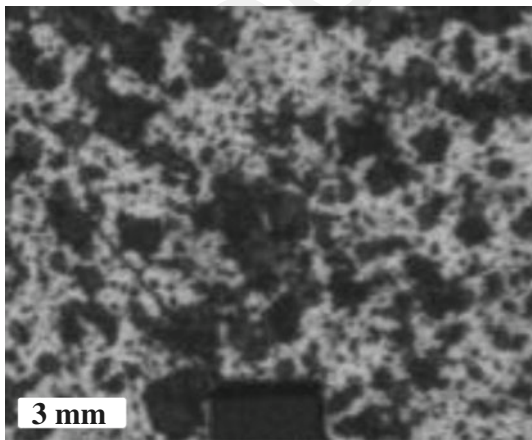


Fig. 5 Typical mode II crack pattern observed on painted graphitized carbon cathode

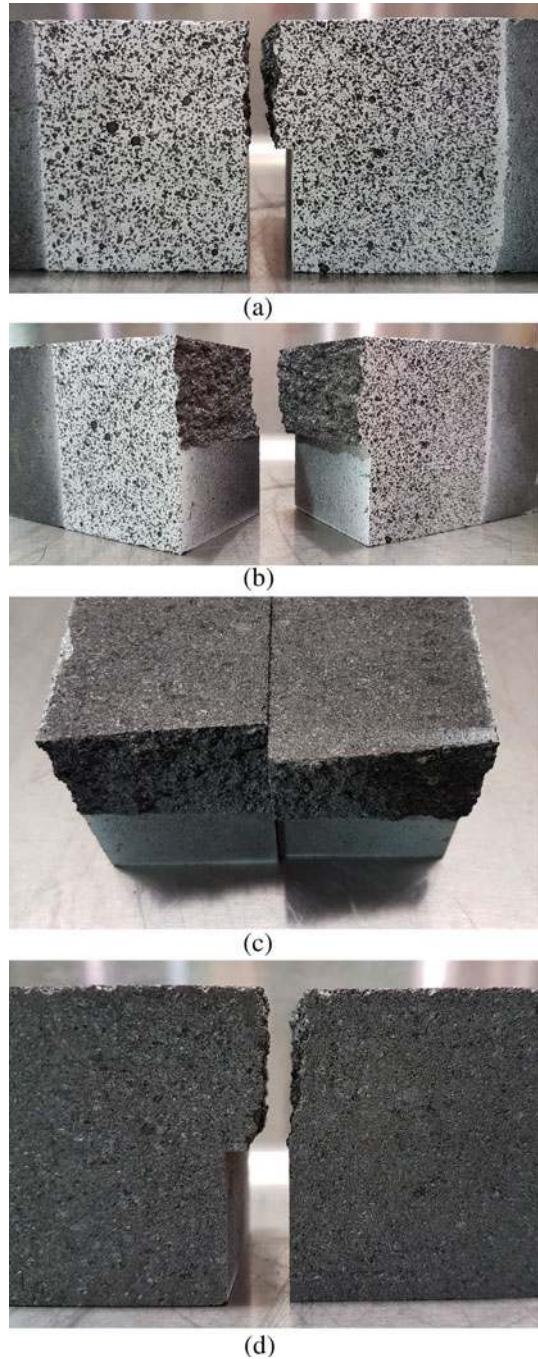


Fig. 6 Typical mode I cracked sample after a stress intensity factor test. **a** front view; **b** open view; **c** side by side view; **d** rear view

As expected for a mode I fracture mechanism, the horizontal and vertical displacements are mostly symmetrical far from the crack. In this latter region, displacements are of course affected by the crack propagation. However, as mentioned previously, this displacement field may vary through the width of the sample (see Fig. 6).

The crack length evolution of both samples SIF-I-01 and SIF-I-02 are shown in Fig. 9. It can be seen that the crack

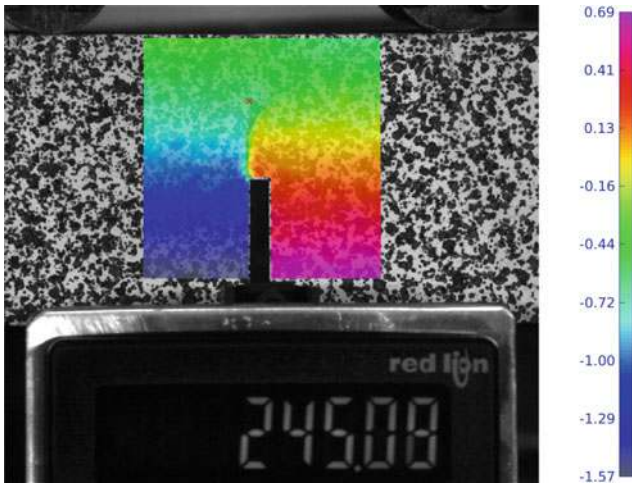


Fig. 7 Horizontal displacement field (mm) of sample SIF-I-01 after 245.08 s

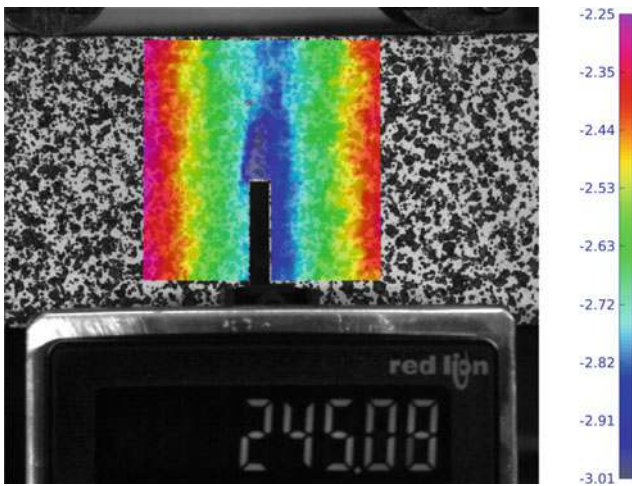


Fig. 8 Vertical displacement field (mm) of sample SIF-I-01 after 245.08 s

evolution in this cathode material is not a monotonous one. Two similar events can be observed after approximately 212 s and 219 s in the crack evolution of sample SIF-I-01. At these steps, the crack length increase rapidly. A similar event occurred in sample SIF-I-02 after 210 s. This suggest that at that moment the crack has gone through a weak zone probably containing more graphitized aggregates with planes aligned with the crack direction [3, 20].

Stress Intensity Factors

The stress intensity factor evolution with time of both samples SIF-I- 01 and SIF-I- 02 is shown in Fig. 10. Contrary to the observations on crack length evolutions (Fig. 9), there are no clear events related to crack propagation in

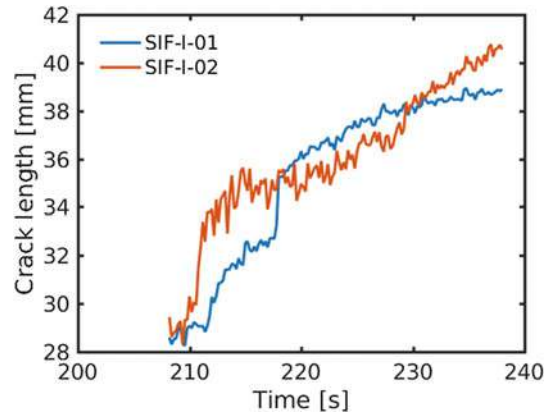


Fig. 9 Crack length evolution of samples SIF-I-01 and SIF-I-02 as a function of time

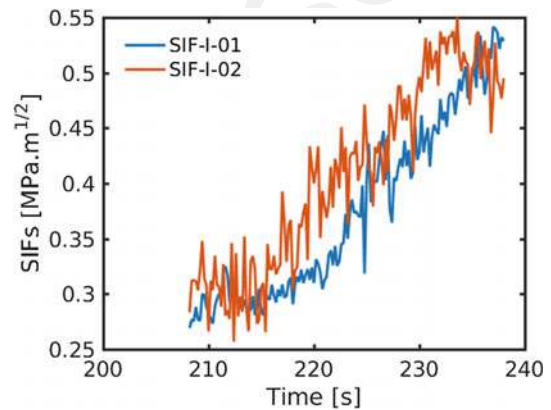


Fig. 10 Stress intensity factor K1 evolution of samples SIF-I-01 and SIF-I-02 with time

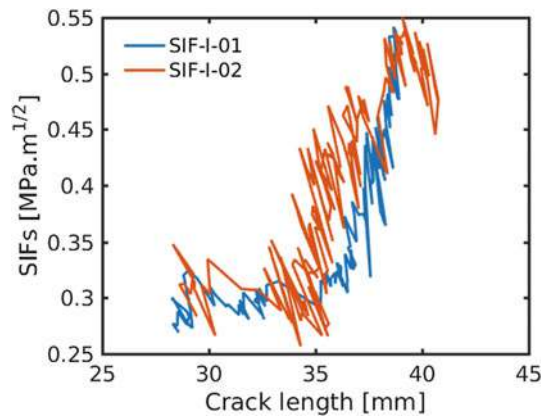


Fig. 11 Stress intensity factor K1 evolution of samples SIF-I-01 and SIF-I-02 as a function of crack length

weaker zones Instead, the Stress Intensity Factors seem to increase almost monotonously with time. This is not the case when Stress Intensity Factors K1 are compared to crack lengths as shown in Fig. 11. In both samples, K1 is almost

constant up to a crack length of about 35 mm. After that, Stress Intensity Factors K_I increase almost with a constant slope up to a crack length of about 40 mm. This seems to indicate that for those two tests weak zones are located roughly at the same distance from the initial notch and that they have almost the same size in both samples. Even though graphitized carbon cathodes are heterogeneous and the SIF extraction ignores the presence of these heterogeneities, the critical stress intensity factor for the weak zones seems to be reproducible at $SIF \sim 0.3 \text{ MPa} \cdot \sqrt{\text{m}}$.

Conclusion

Cracking behaviour has been characterized through the stress intensity factors K_I related to normal (mode I) stress. This factor has been calculated based on displacement field obtained with a Digital Image Correlation method during four-point bending tests of notched cathode samples. Sample heterogeneity effect on cracking behaviour has been highlighted and justified the need to have a large number of tests in order to identify the mode I fracture behaviour. As expected, cracking seems to be highly affected by the presence of carbon aggregates with planes aligned with the cracking direction. Nevertheless, the evolution of the stress intensity factor K_I as a function of the crack length indicated that flexural tests on notched specimen where only mode I is solicited are reproducible. Finally, critical stress intensity factor for the weak zones seems to be reproducible at $SIF \sim 0.3 \text{ MPa} \cdot \sqrt{\text{m}}$.

Acknowledgements Authors would like to acknowledge the financial support of Natural Sciences and Engineering Research Council (NSERC). A part of the research presented in this paper was financed by the Fonds de Recherche du Québec-Nature et Technologie (FRQNT) by the intermediary of the Aluminium Research Centre-REGAL.

References

1. M. Sørli, H.A. Øye, Cathode in aluminium electrolysis. 3rd edn (Aluminium-Verlag Marketing & Kommunikation GmbH, Düsseldorf, Germany, 2010)
2. B. Allard, J.-M. Dreyfus, M. Lenclud, Evolution of thermal, electrical and mechanical properties of graphitised cathode blocks for aluminium electrolysis cells with temperature. *Light Metals* (2000)
3. B. Allard et al., High temperature mechanical behaviour of carbon materials used in aluminium smelters. *Light Metals*, 783–790 (1995)
4. D. Dumas, P. Lacroix, High temperature measurement of electrical resistivity and thermal conductivity on carbon materials used in aluminium smelters. *Light Metals*, 751–760 (1994)
5. A.A. Mirchi, W. Chen, M. Tremblay, Comparative characterisation of graphitized and graphitic cathode blocks. *Light Metals* (2003)
6. D. Picard et al., Thermo-Mechanical characterisation of graphitic and graphitized carbon cathode materials used in aluminium electrolysis cells. *Light Metals* (2010)
7. T.L. Anderson, *Fracture mechanics: fundamentals and applications*, 621 p (2005)
8. Wikipedia. Stress intensity factor. Available from: https://en.wikipedia.org/wiki/Stress_intensity_factor
9. A.F. Bower, *Appl. Mech. Solid.* p. xxv, 794 p (2010)
10. P. Leplay et al., Identification of damage and cracking behaviours based on energy dissipation mode analysis in a quasi-brittle material using digital image correlation. *Int. J. Fract.* **171**(1), 35–50 (2011)
11. F. Rajabipour, H. Maraghechi, G. Fischer, Investigating the Alkali-Silica reaction of recycled glass aggregates in concrete materials. *J. Mater. Civ. Eng.* **22**(12), 1201–1208 (2010)
12. S.Y. Alam, A. Loukili, F. Grondin, Monitoring size effect on crack opening in concrete by digital image correlation. *Eur. J. Environ. Civ. Eng.* **16**(7), 818–836 (2012)
13. D. Corr et al., Digital image correlation analysis of interfacial debonding properties and fracture behavior in concrete. *Eng. Fract. Mech.* **74**(1–2), 109–121 (2007)
14. Y. Duhamel-Labrecque et al., Featuring the micro-cracking process of uhpfc under bending by digital image correlation. *Am. Concr. Inst. J. Mater.* M2016–163 (2016)
15. ISO Standard 18515:2007, Carbonaceous materials for the production of aluminium—cathode blocks and baked anodes—determination of compressive strength, ISO International Standard, Switzerland (2007)
16. ASTM Standard C695—91, 2010, Standard Test Method for Compressive Strength of Carbon and Graphite, ASTM International, West Conshohocken, PA, 2010. doi:10.1520/C0695-15
17. ASTM Standard C469, 2014, Standard Test Method for Static Modulus of Elasticity and Poisson's Ratio of Concrete in Compression, ASTM International, West Conshohocken, PA, 2014. doi:10.1520/C0469_C0469M
18. ASTM Standard C496/C496 M – 11, 2011, Standard Test Method for Splitting Tensile Strength of Cylindrical Concrete Specimens, ASTM International, West Conshohocken, PA, 2011. doi:10.1520/C0496_C0496M-11
19. ASTM Standard C651, 2015, Standard Test Method for Flexural Strength of Manufactured Carbon and Graphite Articles Using Four-Point Loading at Room Temperature, ASTM International, West Conshohocken, PA, 2015. doi:10.1520/C0651-15
20. F. Durand et al., Characterization of the high temperature mechanical behavior of carbon materials. *Carbon* **32**(5), 857–865 (1994)